# Transformation optics for the validation of a time-domain full-wave model of linear complex media

Abdelrahman Ijjeh, Michel Ney

# Transformation optics for the validation of a time-domain full-wave model of linear complex media

A. Ijjeh[1] · M. M. Ney[1]

**Abstract** Complex media have gained interest in microwave and millimeter-wave devices. They display some interesting characteristics such as, for instance, tunability and controlled filtering capacity. However, such media are generally very complex as they can be fully nonhomogeneous; frequency dependent, anisotropic, time dependent, or chiral. This requires simulation techniques capable of solving Maxwell's equations accounting for such media. Also, apart comparison with rather difficult measurement, canonical solutions are not available for validation. In this paper, the concept of transformation optics (TO) is presented as a systematic tool to construct computational problems involving complex media for which the analytical solution is known. Several examples are shown for validation of a new transmission-line matrix (TLM) cell that model complex media.

**Keywords** Transformation optics · Complex linear media · Coordinate transformation · Transmission line matrix method (TLM) · Full-wave methods

## 1 Introduction

Simple electrodynamic problem usually includes media that are defined by three electromagnetic parameters, namely, permittivity, permeability, and conductivity; all of them are positive constant scalars [1]. However, if any of these parameters violate the above assumption, the material is said to be complex. The complexity of the linear medium can manifest itself by possessing one or more properties such as inhomogeneity, dispersion, anisotropy, chirality, time varying, etc. [2].

✉ A. Ijjeh
abdelrhaman.ijjeh@telecom-bretagne.eu

[1] Mines-Telecom Institute, Telecom Bretagne, 29238 Brest cedex 3, France

An important issue that appears once we develop an electromagnetic (EM) simulator that can handle such complex media is to test and validate this solver. This can be a very difficult task due to the lack of analytical canonical examples that include general complex media in the literature.

In this paper, we present the concept of transformation optics as a systematic procedure for constructing computational problems including linear complex media, for which the analytical solutions are known. This technique is based on transforming a computational problem including simple media in an original computational coordinate system, into a new computational problem including complex media in a new coordinate system.

In Section 2, we present the mathematical basis of this approach. In Section 3, we present three numerical experiments for computational domains containing complex media to show the validity of the TLM model [3] for complex media. For comparison, analytical solutions are considered as references.

## 2 Mathematical model

### 2.1 Evolution equations for complex linear media

Maxwell's equations for general linear dispersive media which can be written in time domain as [2, 3]:

$$\begin{pmatrix} \nabla \times H \\ -\nabla \times E \end{pmatrix} - \begin{pmatrix} J_{ef} \\ J_{mf} \end{pmatrix} = \frac{\partial}{\partial t} \begin{pmatrix} \varepsilon_o E \\ \mu_o H \end{pmatrix} + \begin{pmatrix} \overline{\overline{\sigma}}_e * E \\ \overline{\overline{\sigma}}_m * H \end{pmatrix} + \frac{\partial}{\partial t} \begin{pmatrix} \varepsilon_o \overline{\overline{\chi}}_e & \frac{\overline{\overline{\xi}}}{c_o} \\ \frac{\overline{\overline{\zeta}}}{c_o} & \mu_o \overline{\overline{\chi}}_m \end{pmatrix} * \begin{pmatrix} E \\ H \end{pmatrix} \quad (1)$$

where $\overline{\overline{\chi}}_e$ and $\overline{\overline{\chi}}_m$ are the electric and magnetic susceptibility tensors, respectively, $\overline{\overline{\sigma}}_e$, $\overline{\overline{\sigma}}_m$ are the electric and magnetic conductivities tensors, $\overline{\overline{\xi}}$ and $\overline{\overline{\zeta}}$ are the chirality (the electromagneto coupling factors [3]) tensors, respectively, and * is the time domain convolution process.

### 2.2 Mapping computational problems between different coordinate systems

Transformation optics is a collection of theory that governs the mapping of computational problems in one domain (with specific coordinate system) into another one in a different coordinate system [4, 5]. This provides us with mathematical tools to study the same computational problem in different coordinate systems. However, any change in the coordinate system will directly impact on the media properties inside the computational domain as shown in Fig. 1.

In general, after applying the coordinate transformation $\phi$, two impacts on the original computational domain occur:

The geometry changes according to the map of coordinate transformation $\phi$.

The material property tensors are modified according to the Jacobian $\Lambda$ of the transformation $\phi$ as presented in Table 1.

## 3 Results and discussions

In this section, we present three numerical experiments to show the validity of our approach where we used TLM numerical method to do the simulations. In all experiments, we show the results of the problem in the original computational domain, the transformed domain, and compare with the analytical solutions.

### 3.1 Rotation of a PEC cylindrical cavity

In this example, we exploit the previously mentioned procedure to create an example of a structure that contains anisotropic media with non-diagonal tensor. The analytical solution of this example is already known and will be used for comparisons with numerical results obtained by an electromagnetic solver developed on TLM [3].

Initially, we consider a perfectly conducting (PEC) cylindrical cavity of radius 18 mm and height of 6 mm filled by an anisotropic medium defined by the following constitutive parameters:

$$\overline{\overline{\varepsilon}}_r = \begin{pmatrix} \varepsilon_x & 0 & 0 \\ 0 & \varepsilon_y & 0 \\ 0 & 0 & \varepsilon_z \end{pmatrix} \quad ; \quad \overline{\overline{\mu}}_r = \begin{pmatrix} \mu_x & 0 & 0 \\ 0 & \mu_y & 0 \\ 0 & 0 & \mu_z \end{pmatrix} \tag{2}$$

Now, one applies the following coordinate transformation (rotation around the $z$-axis):

$$\begin{pmatrix} x' \\ y' \\ z' \end{pmatrix} = \begin{pmatrix} \cos(\phi) & -\sin(\phi) & 0 \\ \sin(\phi) & \cos(\phi) & 0 \\ 0 & 0 & 1 \end{pmatrix} \begin{pmatrix} x \\ y \\ z \end{pmatrix} \tag{3}$$

According to the rules of Table 1, one can obtain the permittivity and permeability expression in the new coordinate system:

$$\overline{\overline{\varepsilon}} = \begin{pmatrix} \cos^2(\phi)\,\varepsilon_x + \sin^2(\phi)\,\varepsilon_y & \sin(\phi)\cos(\phi)\varepsilon_y - \sin(\phi)\cos(\phi)\varepsilon_x & 0 \\ \sin(\phi)\cos(\phi)\varepsilon_y - \sin(\phi)\cos(\phi)\varepsilon_x & \sin^2(\phi)\,\varepsilon_x + \cos^2(\phi)\,\varepsilon_y & 0 \\ 0 & 0 & \varepsilon_z \end{pmatrix} \tag{4a}$$

$$\overline{\overline{\mu}} = \begin{pmatrix} \cos^2(\phi)\,\mu_x + \sin^2(\phi)\,\mu_y & \sin(\phi)\cos(\phi)\mu_y - \sin(\phi)\cos(\phi)\mu_x & 0 \\ \sin(\phi)\cos(\phi)\mu_y - \sin(\phi)\cos(\phi)\mu_x & \sin^2(\phi)\,\mu_x + \cos^2(\phi)\,\mu_y & 0 \\ 0 & 0 & \mu_z \end{pmatrix} \tag{4b}$$

In reality, nothing has changed (just rotating the cylinder around its axis). However, if one looks from the new coordinate system perspective, it is possible to use the new material properties (4a) and (4b) and maintain the same geometry (because of its invariance with the ϕ angle).

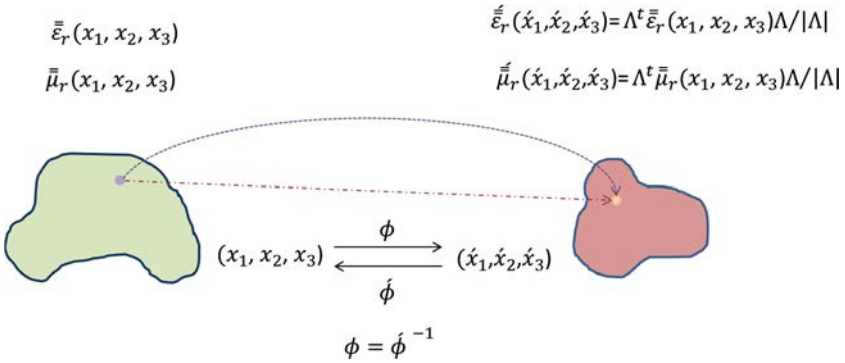


**Fig. 1** Mapping between different coordinate systems

**Table 1** Transformation optic formulas

| Computational domain quantity | Original coordinate system $(x_1, x_2, x_3)$ | Transformed coordinate system $(x_1', x_2', x_3')$ |
|---|---|---|
| Position of a point | $(x_1, x_2, x_3)$ | $\phi(x_1, x_2, x_3) = (x_1', x_2', x_3')$ |
| Permittivity tensor | $\overline{\overline{\varepsilon}}_r$ | $\overline{\overline{\varepsilon}}_r' = \Lambda^t \overline{\overline{\varepsilon}}_r' \Lambda / \det(\Lambda)$ |
| Permeability tensor | $\overline{\overline{\mu}}_r$ | $\overline{\overline{\mu}}_r' = \Lambda^t \overline{\overline{\mu}}_r' \Lambda / \det(\Lambda)$ |
| Conductivity | $\overline{\overline{\sigma}}_r$ | $\overline{\overline{\sigma}}_r' = \overline{\overline{\sigma}}_r \Lambda^t \overline{\overline{\varepsilon}}_r \Lambda / \det(\Lambda)$ |
| Electric current density | $\vec{J}$ | $\vec{J}' = \Lambda^t \vec{J} / \det(\Lambda)$ |
| Electric charge density | $\rho_{ev}$ | $\rho_{ev}' = \rho_{ev} / \det(\Lambda)$ |
| Electric field | $\vec{E}$ | $\vec{E}' = \Lambda' \vec{E}$ |
| Magnetic field | $\vec{H}$ | $\vec{H}' = \Lambda' \vec{H}$ |

As an example, we assume that the cylindrical cavity is filled by an anisotropic medium with the following diagonal tensors (original state before rotation):

$$\overline{\overline{\varepsilon}}_r = \begin{pmatrix} 3 & 0 & 0 \\ 0 & 1 & 0 \\ 0 & 0 & 2 \end{pmatrix} \quad ; \quad \overline{\overline{\mu}}_r = \begin{pmatrix} 3 & 0 & 0 \\ 0 & 1 & 0 \\ 0 & 0 & 2 \end{pmatrix} \tag{5}$$

In this experiment, we used a regular mesh with cubic cells. To maintain a negligible level of numerical dispersion, we used the cell size $\Delta l = 0.3$ mm ($\lambda_0/50$) which provides a sufficiently fine discretization to minimize the stair-case effect and to maintain a negligible level of dispersion. To limit the cylinder volume, we used PEC cubic cells at its boundaries. Consequently, the time step used was $\Delta t = 0.5$ *ps*. For time excitation, one applied a delta Dirac's function at a random point inside the cavity with a polarization in z-direction, and we ran the experiment for 20,000 iterations until the modes were established. Note that in the original system, cylinder rotations do not change the mode resonance values. Thus, resonant frequencies are computed analytically for reference and with the TLM as $\Lambda$ is the identity matrix for 0° angle only in the original domain. However, if the resonance values are constant with the rotation angle, $\Lambda$ differs from identity matrix for other angles in the transformed domain. Also, note that excitations are also transformed according to Table 1. However, it is not relevant for eigenvalue problems as modes are independent on the excitation as long as they can be excited.

Table 2 shows a comparison of the first resonant modes for different rotation angles as compared to the analytical solution known for the cavity filled by the medium characterized by tensors in (5).

As we can see, results produced by the TLM solver are very accurate. Hence, these results validate that the solver is working correctly in case of non-diagonal tensor of an anisotropic media.

### 3.2 Deformation of a PEC spherical resonator

In this numerical experiment, we use TO to verify again the accuracy of the TLM model for another complex media. Consider the conducting sphere of radius 15 cm, as shown in Fig. 2a, filled by a simple nonmagnetic dielectric with $\varepsilon_r = 2.0$.

Now, we assume that the sphere is deformed to the ellipsoid shown in Fig. 2b according to the following coordinate transformation:

$$\begin{pmatrix} x' \\ y' \\ z' \end{pmatrix} \rightarrow \begin{pmatrix} 2x \\ y \\ z \end{pmatrix} \tag{6}$$

**Table 2** Resonant frequencies for the first 4 modes with angles of rotation

| Resonance mode | Rotational angle | 0° | 30° | 45° | 60° | 90° |
|---|---|---|---|---|---|---|
| | | Relative Error% | | | | |
| First mode | | 0.023 | 0.093 | 0.37 | 0.265 | 0.230 |
| Second mode | | 0.109 | 0.563 | 0.647 | 0.395 | 0.059 |
| Third mode | | 0.084 | 0.240 | 0.305 | 0.305 | 0.045 |
| Fourth mode | | 0.011 | 0.094 | 0.063 | 0.063 | 0.011 |

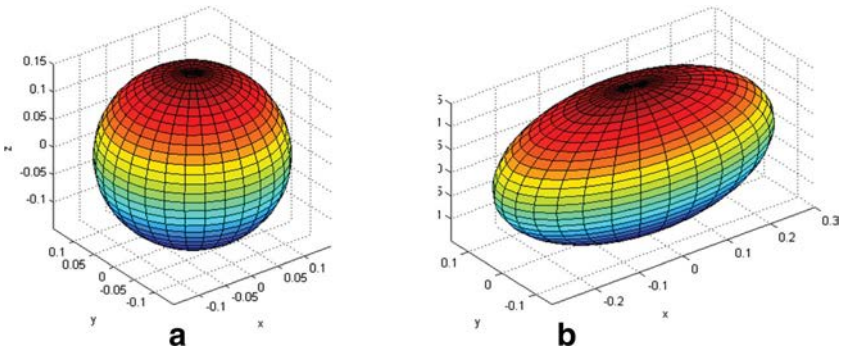


**Fig. 2** **a** spherical PEC resonator filled by an isotropic dielectric, **b** elliptical PEC resonator filled by an anisotropic dielectric medium

This coordinate transformation modifies the material properties as shown in Table 1. Hence, the permittivity and permeability tensors become, respectively:

$$\overline{\overline{\varepsilon}}_r' = \begin{pmatrix} 4 & 0 & 0 \\ 0 & 1 & 0 \\ 0 & 0 & 1 \end{pmatrix} \quad ; \quad \overline{\overline{\mu}}_r' = \begin{pmatrix} 2 & 0 & 0 \\ 0 & 1/2 & 0 \\ 0 & 0 & 1/2 \end{pmatrix} \tag{7}$$

If we simulate an ellipsoid filled by this anisotropic (both dielectric and magnetic) material, we should get the same resonant frequencies as the original problem of the sphere before the deformation.

To perform the numerical experiments for both the elliptical and the spherical cavities described above, we used regular mesh of cubic cells. To maintain a negligible level of numerical dispersion, the cell size is $\Delta l = 3.3$ mm which is equivalent to 23 cells per wavelength with $\varepsilon_r = 2.0$ (relative error less than 1.0 % according to [6]). Moreover, this fine discretization was necessary to reduce the stair-case approximation for both structures. Note that a more complex procedure can be carried out to optimize the maximum cell size to be used for the transformed sphere anisotropic medium [6, 7]. However, for the purpose of this paper, it is not necessary. Thus, we used a finer mesh than necessary to make sure that dispersion is negligible in both systems. The corresponding time steps we used were 5.49 and 2.772 ps for the spherical and the elliptical cavities, respectively. The time excitation applied was a delta function at a random point inside the cavity with a polarization in z-direction, and we run the experiment for 6000 iterations until the modes were established. The number of cells we used for the spherical cavity experiment was 753,571 cells and 1,507,142 cells for the elliptical one.

Table 3 shows a comparison between the numerical results of resonant frequencies calculated for the sphere filled by the isotropic media, the ellipsoid filled by the anisotropic media, and the analytical solution (of the spherical resonator) [8]. We can observe some very good matching between the three cases. This shows the validity of the TLM solver when dealing with anisotropic media.

### 3.3 Shrinking a dielectric slab in a parallel plate waveguide

In this numerical experiment shown in Fig. 3a, b, we compute the reflection and transmission coefficients from a lossless dielectric slab in a parallel-plate waveguide. In both cases, dielectric slab was excited by a TEM plane wave. To obtain a perfect plane wave, the computational domain was terminated by two parallel PEC walls from the top and bottom and two parallel PMC walls at both sides. This will ensure a TEM mode of propagation and generate a one-dimensional electromagnetic problem.

In the first scenario, we performed a numerical experiment with a simple nonmagnetic dielectric layer of permittivity $\overline{\overline{\varepsilon}}_r = 10.0\,\overline{\overline{I}}_3$ and thickness $d = 10.0$ cm (Fig. 3a). Then, we applied the TO coordinate transformation in which we shrink

**Table 3** Comparison between spherical and elliptical resonators with the analytical solution

| Resonant modes | Elliptical resonator (GHz) | Relative error% | Spherical resonator (GHz) | Relative error% | Analytical solution (GHz) |
|---|---|---|---|---|---|
| First mode | 1.329 | 0.24 | 1.321 | 0.36 | 1.3258 |
| Second mode | 1.866 | 0.21 | 1.863 | 0.37 | 1.8699 |
| Third mode | 2.184 | 0.60 | 2.172 | 0.05 | 2.1709 |
| Fourth mode | 2.399 | 0.16 | 2.390 | 0.54 | 2.4029 |
| Fifth mode | 2.810 | 0.91 | 2.791 | 0.23 | 2.7846 |

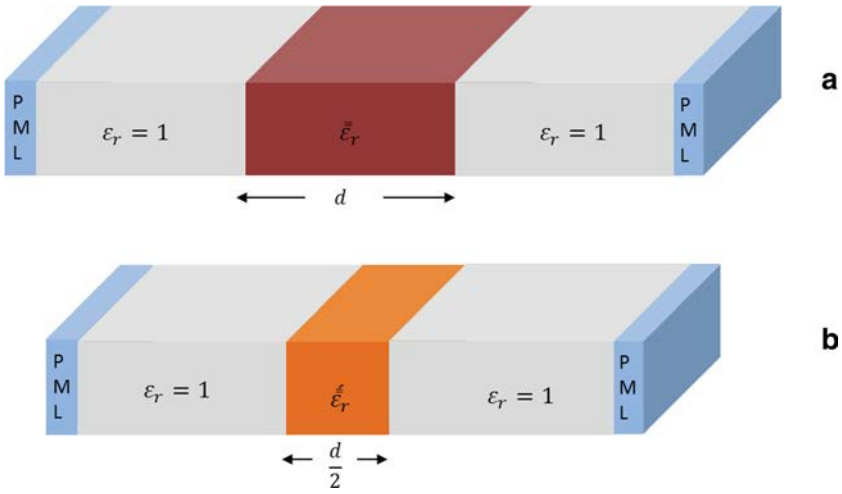


**Fig. 3** Scattering problem in parallel plate waveguide, **a** original computational domain with simple media, **b** transformed computational domain with complex media

only the dielectric layer to $d/2 = 5.0$ cm (Fig. 3b). This results in a new computational domain in which the dielectric layer has permittivity and permeability given by:

$$\bar{\bar{\varepsilon}}'_r = \begin{pmatrix} 20 & 0 & 0 \\ 0 & 20 & 0 \\ 0 & 0 & 5 \end{pmatrix} \quad ; \quad \bar{\bar{\mu}}'_r = \begin{pmatrix} 2 & 0 & 0 \\ 0 & 2 & 0 \\ 0 & 0 & 1/2 \end{pmatrix} \tag{8}$$

In this numerical experiment, we used regular mesh of cubic cells. To maintain a negligible level of numerical dispersion, we used the cell size to be $\Delta l = 5$ mm, which is equivalent to 27 cells per wavelength in the isotropic medium of the original domain before transformation. Consequently, the time step we used is $\Delta t = 4.0\ ps$. The time excitation was a modulated Gaussian pulse at center frequency $f_o = 0.5$ GHz and parameters $\sigma = 30\Delta t$ and $t_o = 300\Delta t$. The experiment was performed for 9000 iterations until the all the fields vanished from the computational domain.

Figures 4 and 5 show the reflection and transmission coefficients, respectively, over the frequency range from 250 to 700 MHz. As expected, we can see some good matching between both TLM simulations (the original and transformed domain) with the analytical solution [9]:

$$S_{11} = \frac{Z_{in} - Z_o}{Z_{in} + Z_o} \tag{9a}$$

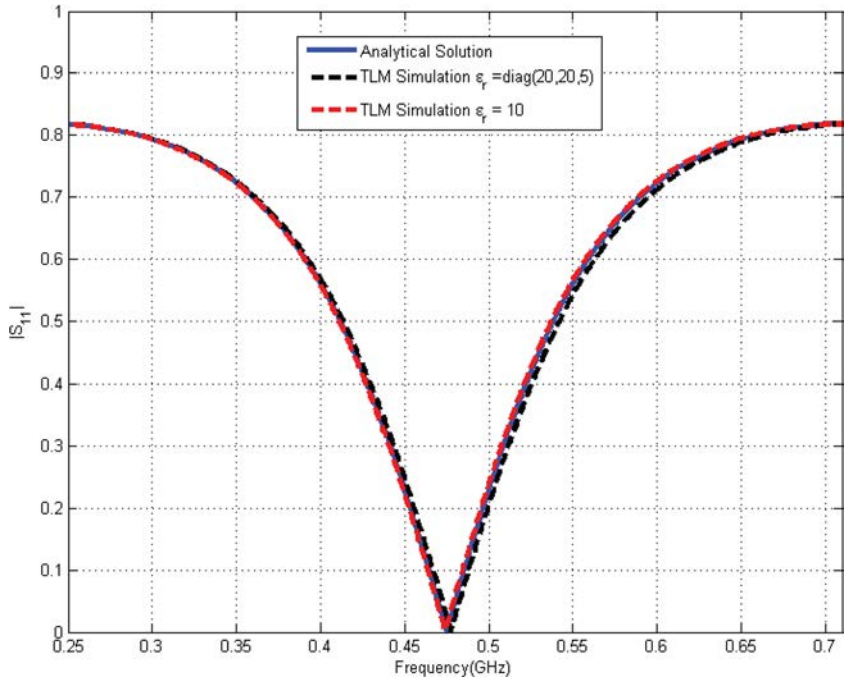


**Fig. 4** Reflection coefficient: a comparison between analytical solution and TLM algorithm for both original computational domain and transformed domain

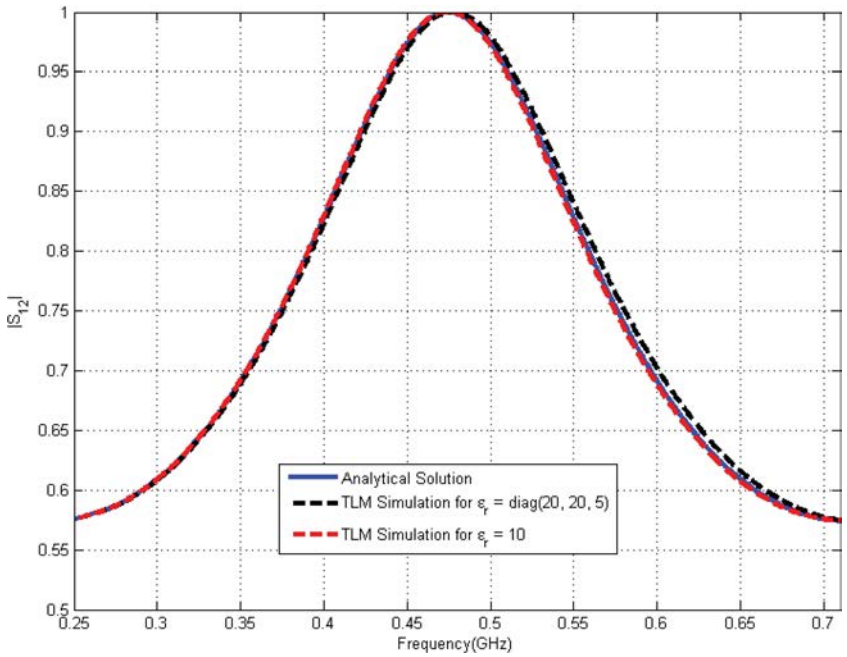


**Fig. 5** Transmission coefficient: a comparison between analytical solution and TLM algorithm for both original domain and transformed computational domain

where the input impedance is defined as:

$$Z_{in} = Z_o \sqrt{\frac{\mu_r}{\varepsilon_r}} \left( \frac{1 + \sqrt{\frac{\mu_r}{\varepsilon_r}} j tan(\beta d)}{\sqrt{\frac{\mu_r}{\varepsilon_r}} + j tan(\beta d)} \right) \tag{9b}$$

where $Z_o$ is the wave impedance in free space, $\mu_r$ and $\varepsilon_r$ are the permeability and permittivity of the dielectric slab in the original domain (Fig. 3a), $\beta$ is the wave number inside the isotropic dielectric slab, and $d$ is the thickness of the dielectric slab shown in Fig. 3a.

We can notice that the results obtained in the transformed domain have some higher (but still very small) discrepancy with the analytical solution than the results obtained in the original domain. This observation is expected since we used the same cell size for both original and transformed domains. In fact, the anisotropic media [6, 7] acquire higher dispersion characteristics than isotropic media. Finally, one can conclude that these results validate the solver correct functionality for media having diagonal tensors constitutive parameters. They also validate the approach using TO.

## 4 Conclusion

A systematic procedure based on transformation optics was presented that allows one to construct computational problems that include complex media for which we know the analytical solution. This procedure was tested with several cases and allowed us to validate the numerical model under consideration (TLM model in our case). In all experiments that have been presented, fine meshes were used to ensure minimal dispersion for both domains. More complicated coordinate transformations can be used to obtain more complex media properties, for instance, one can use time-varying coordinate systems to obtain dispersive media.

## References


1. D. K. Kalluri (2010) Electromagnetics of Time Varying Complex Media, CRC Press
2. L. Landau and E. M. Lifshitz (1984) Electrodynamcis of Continuous Media, Pergamon Press
3. Farhat AL, Maguer SL, Quéffélec P, Ney M (2012) TLM extension to electromagnetic field analysis of anisotropic and dispersive media: a unified field equation. IEEE Trans Microwave Theory Tech 60(8): 2339–2351
4. Ward AJ, Pendry JB (1996) Refraction and geometry in Maxwell's equations. J Mod Opt 43(4):773–793
5. Kundtz NB, Smith DR, Pendry JB (2011) Electromagnetic design with transformation optics. Proc IEEE 99(10):1622–1633
6. A. Ijjeh, M. M. Ney and F. Andriulli (2016) Dispersion Analysis in Time-Domain Simulation of Complex Dispersive Media. IEEE-MTT Int. Conf. On Numerical Electromagnetic and Multiphysics Modeling and Optimization, NEMO 2016, Ottawa, Aug. 11-14
7. Huber C, Krumpholz M, Russer P (1995) Dispersion in aniotropic media modeled by three-dimensional TLM. IEEE Trans Microwave Theory Tech 43(8):1923–1934
8. J. D. Jackson (1999) Classical Electrodynamics. Wiley
9. D. Pozar (2009) Microwave engineering. Wiley